Identification of GaN Buffer Traps in Microwave Power AlGaN/GaN HEMTs Through Low Frequency S-Parameters Measurements and TCAD-Based Physical Device Simulations

Nandha Kumar Subramani, Julien Couvidat, Ahmad Al Hajjar, Jean-Christophe Nallatamby, Raphaël Sommet, Raymond Quéré

Received 17 December 2016; revised 6 February 2017; accepted 14 February 2017. Date of publication 20 March 2017;
date of current version 24 April 2017. The review of this paper was arranged by Editor C. Surya.

Digital Object Identifier 10.1109/JEDS.2017.2672685

Identification of GaN Buffer Traps in Microwave Power AlGaN/GaN HEMTs Through Low Frequency S-Parameters Measurements and TCAD-Based Physical Device Simulations

NANDHA KUMAR SUBRAMANI, JULIEN COUVIDAT, AHMAD AL HAJJAR, JEAN-CHRISTOPHE NALLATAMBY, RAPHAEL SOMMET, AND RAYMOND QUÉRÉ (Fellow, IEEE)

University of Limoges, CNRS, XLIM, UMR 7252, F-19100 Brive, France

CORRESPONDING AUTHOR: N. K. SUBRAMANI (e-mail: nandhakumar2005@gmail.com)

This work was supported by DEFIS-RF Project, France, under Contract ANR 13-CHN-0003.

ABSTRACT In this paper, the type, activation energy (E_a) and cross section (σ_n) of the GaN buffer traps existing in the AlGaN/GaN high-electron mobility transistors are investigated through low frequency (LF) S-parameters measurements. Furthermore, we present the 2-D physics based TCAD numerical simulation analysis of this device. The dc simulation results are calibrated to match with the experimentally measured *I–V* characteristics and this allows to qualitatively estimate the concentration of traps (N_T) present in the GaN buffer. Knowing the measured trap energy level and the estimated trap concentration N_T, TCAD physical simulations are performed at various temperatures in order to extract the LF-Y_{22} admittance parameter. Interestingly, the LF-Y_{22} simulation results are found to be in good agreement with the measurements and this result strongly suggests that LF admittance dispersion is an effective tool in identifying the traps present in the GaN buffer. Moreover, this paper reveals that acceptor-like traps with an apparent concentration of 5.0×10^{16} cm^{-3} and with the apparent trap energy level of 0.4 eV below the conduction band are located in the GaN buffer.

INDEX TERMS Gallium-nitride (GaN), high electron mobility transistor (HEMT), buffer traps, TCAD simulation, low frequency S-parameters.

I. INTRODUCTION

In recent years, GaN material receives significant attention due to its superior material properties [1], [2] such as wide bandgap, high electron mobility, high saturation velocity and high breakdown electric field. Moreover, there has been tremendous development focused on the growth of GaN high electron mobility transistor (HEMT) device technology including improving the material quality of epitaxial [3] and passivation layers [2], selecting the appropriate substrate materials [3], [4] implementing the field plates [2], [5] and ultra-short gate lengths [6], [7] and optimizing the AlGaN barrier thickness [6]. All these technological improvements enabled GaN HEMT technology as a disruptive technology for high-power microwave and mm-wave applications [8]. Furthermore, GaN HEMT device is capable of delivering high breakdown voltage, high switching speed and low on-resistance (R_{ON}), which makes it ideal for power switching applications [9].

Although GaN HEMT devices have demonstrated their superior performance [3], [6], the presence of deep levels in the structure degrades the dynamic device performance [10] Indeed, the density of two-dimensional electron gas (2DEG) at the heterostructure interface is altered due to the capture of electrons by the deep levels either present at the surface, or barrier or buffer layer [10]. Moreover, these traps are slow in nature and thus undermines the device reliability [11], [12]. Several types of trapping effects have been reported in [9]–[11]. However, the origin and properties of these traps remain unclear. Trapping effects causes current collapse – a recoverable reduction in drain current after the application of high biasing voltage, transconductance-frequency dispersion, gate lag, drain lag, and restricted microwave output

power [9]. Several studies have also demonstrated that the presence of Fe-doped GaN buffer causes enhanced current collapse mechanism [13] and thereby deviates from expected microwave performance. Therefore, the analysis of traps and identifying the ways to minimize the trapping effects is an active research area to explore. There are various measurement techniques [9]–[16], such as deep level transient spectroscopy (DLTS), gate and drain lag transients, high-voltage transient CV, frequency dependent transconductance dispersion and low frequency noise (LFN) measurements are available to investigate the trapping behavior of the GaN HEMT devices.

In this work, traps in the buffer region of a GaN/AlGaN/GaN HEMT transistor grown on SiC substrate have been characterized using low frequency S-parameters measurements [17]. These measurements allow us to determine the activation energy E_a and the cross section σ_n of the traps existing in the GaN buffer. Furthermore, we also present the TCAD physics based DC and LF-Y_{22} simulation results to validate our measurement technique. Our simulation results strongly suggests that LF output admittance measurement technique could be an efficient tool for identifying the traps in the buffer region of GaN HEMT devices. Furthermore, our simulation results insist that traps in the AlGaN barrier cannot be identified using the aforementioned technique. The paper is organized as follows. Section II briefly describes the HEMT device under test and it also discusses the extraction of trap parameters from LF measurements. In Section III, we present results obtained using LF S-parameters measurements. Furthermore, we also describe the physics-based TCAD numerical device simulation approach of GaN/AlGaN/GaN HEMT device and discusses the obtained DC and LF admittance simulation results. Finally, Section IV concludes the paper.

II. TRAP CHARACTERIZATION METHODOLOGY

The GaN/AlGaN/GaN HEMTs were grown by metal-organic chemical vapor deposition (MOCVD) on a SiC substrate. The fabricated transistor has a gate length (L_G) of 0.25 μm and a width, W_G of 600 μm (eight fingers, n = 8), whereas the nominal gate-source (L_{SG}) and gate-drain (L_{GD}) spacings are 0.8 and 2.7 μm, respectively. A field-plate is placed from middle of the gate electrode and extends a distance L_{FP} (field-plate length) of 1 μm towards the drain electrode.

On-wafer pulsed-IV measurements have been carried out by using an AMCAD BILT pulsed IV system. The gate and drain terminals are pulsed at $V_{GSQ} = V_{DSQ} = 0$ V. The measured pulsed I-V characteristics are used to calibrate the TCAD physical simulation model. The corresponding measurement results are presented along with the simulation results in the next section. The low frequency S-parameters measurements in the frequency range of 10 Hz to 10 MHz have been carried out using an Agilent E5061B network analyzer for various thermal chuck (T_{chuck}) between 25°C and 100°C. More details on the measurement configuration used for this work is given in [18]. A standard SOLT method is used to calibrate the network analyzer.

The measured LF S-parameters are converted into their equivalent Y-parameters. The traps in the GaN buffer cause the frequency dispersion in the measured device output admittance Y_{22} parameter. The corresponding emission time (τ_n) of the traps can be calculated from the peak value of imaginary part of the Y_{22} parameter by using (1) [17]:

$$f_{I,peak} = f_{\mathrm{Im}\,ag[Y_{22}]} = \frac{1}{2\pi\tau_n} \tag{1}$$

As the temperature increases, the electron emission rate increases, hence the emission time constant decreases which causes the peak value of Y_{22} parameter shift towards higher frequencies. Therefore, the activation energy (E_a) and cross section (σ_n) of the traps can be determined using the Arrhenius equation (2) [17]:

$$\frac{e_n}{T^2} = \frac{\sigma_n \cdot A_n}{g} \exp\left(-\frac{E_a}{k \cdot T}\right) \tag{2}$$

with

$$A_n = \frac{N_C \cdot V_{th}}{T^2} \text{ and } e_n = \frac{1}{\tau_n}$$

where, e_n is the trap emission rate, T is the temperature, σ_n is the capture cross section of traps, N_C is the effective density of states of electrons in the conduction band, V_{th} is the thermal velocity of electrons, g is the degeneracy factor ($g = 1$), E_a is the trap activation energy and k is the Boltzmann constant.

The emission time constant is calculated at each measurement temperature using (1). Then, by using the Arrhenius equation, the plot of $ln\,(\tau_n T^2)$ versus $1/kT$ yields the straight line, whose slope and intercept determine the apparent activation energy and cross section of the traps existing in the GaN buffer.

III. RESULTS AND DISCUSSIONS

A. EXPERIMENTAL

Fig. 1(a) shows the imaginary part of the Y_{22} parameter extracted using LF S-parameter measurements for the frequency range of 100 Hz to 10 MHz and for the bias conditions of $V_{DS} = 30$ V and $I_D = 57$ mA (deep class AB operation). This operation mode is selected since it is being widely preferred nowadays for designing RFPA. The emission time constant is calculated as a function of temperature from the peak value of imaginary part of Y_{22} using (1). Fig. 1(b) shows the Arrhenius plot of traps extracted using LF measurements. The apparent activation energy and cross section of the traps determined are 0.4 eV and $1.89 \times 10^{-16}\mathrm{cm}^2$, respectively. Therefore, these results confirm that traps exist in GaN buffer with an apparent activation energy of 0.4 eV below the conduction band. The physical origin of this traps could be related to iron doping present in the GaN buffer.

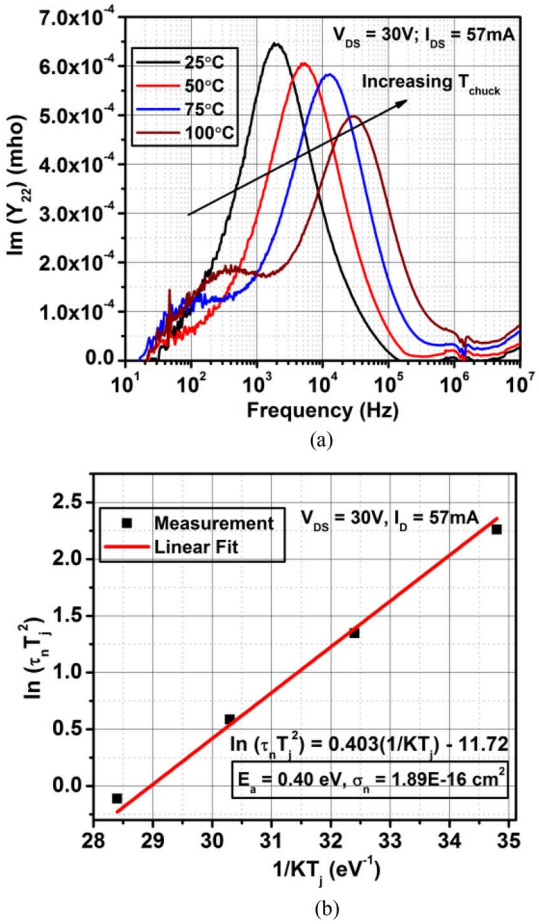

FIGURE 1. **(a) Imaginary part of the measured Y_{22}-parameter vs. frequency for the T_{chuck} ranges between 25°C and 100°C. Bias conditions: V_{DS} = 30 V and I_D = 57 mA. (b) Extracted Arrhenius plot using Y_{22}-parameter.**

TABLE 1. **Summary of the material parameters used in simulations.**

Material property	Units	GaN	AlGaN
Electron Mobility	cm^2/V. s	1200	300
Bandgap	eV	3.50	4.39
Relative permittivity	-	8.9	8.8
Electron affinity	eV	4.0	3.41
Electron saturation velocity	cm/s	2.5×10^7	1.1×10^7
Effective conduction band density of states	cm^{-3}	2.23×10^{18}	2.71×10^{18}
Effective valence band density of states	cm^{-3}	2.51×10^{19}	2.06×10^{19}

B. TCAD PHYSICAL SIMULATION

Two-dimensional physical simulations have been carried out using the commercially available TCAD Sentaurus software from Synopsys Inc. Poisson's equation, and continuity equations for both electrons and holes, and the drift-diffusion (DD) model transport equations are solved self-consistently. The cross section of the structure used for the simulation is shown in Fig. 2 (a). More experimental details on the thickness of each layers of the device cannot

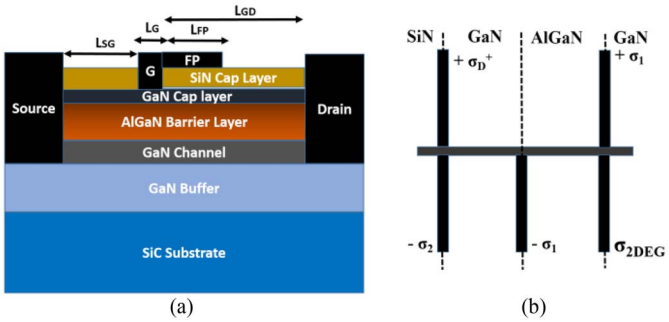

FIGURE 2. **(a) Cross-sectional structure of the simulated GaN/AlGaN/GaN HEMT on SiC substrate. (b) Polarization charges defined in the physical simulation.**

be given due to confidential reasons. The presence of spontaneous and piezoelectric polarization charges induces the electric field in the device structure and this contributes to the formation of 2DEG density at the AlGaN/GaN heterostructure interface, even without the requirements for any intentional AlGaN barrier doping [19]. In absence of any external electric fields, the polarization charges formed are of course, equal in magnitude and opposite in sign to maintain the overall charge neutrality of the device [20]. The polarization charges used in the simulation have been calculated based on the theoretical method given in [19]. Fig. 2(b) shows the polarization charges used at each material interface in the physical simulator. The values of σ_1 and σ_2 are $\pm$ 1.23 $\times$ 10^{13} cm^{-2} and -2.0 $\times$ 10^{12} cm^{-2}, respectively. Moreover, the surface donors are introduced at the GaN/SiN interface in order to form the 2DEG in the channel. Donor-like traps (σ_D^+) with a density of 1.0 $\times$ 10^{13} cm^{-2} and a specified energy level of 0.2 eV below the conduction band are defined. Iron doping (Fe-doped) are introduced in the GaN buffer with a constant concentration of 3.0 $\times$ 10^{16} cm^{-3}. In addition, we consider acceptor-like traps in the GaN buffer whose trap energy is placed at 0.4 eV below the conduction band and the assumed trap concentration is 5.0 $\times$ 10^{16} cm^{-3}. Electron (σ_n) and hole (σ_p) capture cross sections of GaN buffer traps are assumed to be 3.2 $\times$ 10^{-18} and 1.0 $\times$ 10^{-20} cm^2, respectively. For the simulation, constant mobility and field dependent mobility models are included for electrons and holes and Shockley-Read-Hall recombination model is used for carrier generation and recombination. The summary of the material parameters used in our simulations are listed in Table 1.

C. COMPARISON: IDENTIFICATION OF GAN BUFFER TRAPS

The simulation model is calibrated to match with the experimentally measured I-V characteristics. Further details about calibrating the TCAD physical models can be in found in [18]. Fig. 3(a) and 3(b) show the simulated and measured transfer and output characteristics of the device at T_{chuck} = 25°C. Fig. 3(c) shows the comparison of the simulated and measured I_D-V_{DS} characteristics at V_{GS} = 0 V

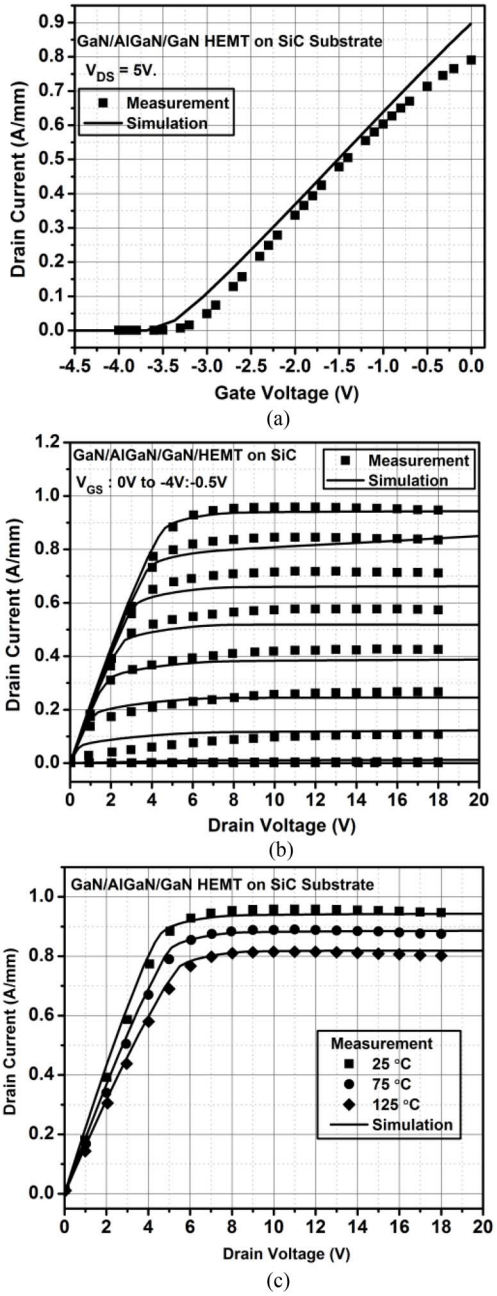

FIGURE 3. Comparison of the simulated (solid lines) and measured (symbols) I-V characteristics. (a) Transfer characteristics at V_{DS} = 5 V and T_{chuck} = 25°C. (b) Output characteristics for varying V_{GS} between 0 V and -4 V in steps of 0.5 V and at T_{chuck} = 25°C. (c) Output characteristics for T_{chuck} varying between 25°C and 125°C and at V_{GS} = 0 V.

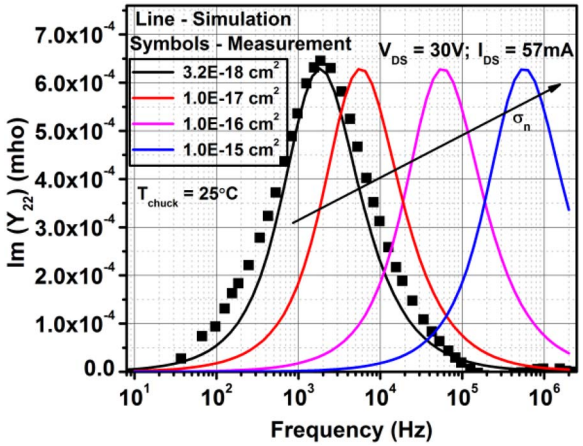

FIGURE 4. Imaginary part of the simulated (lines) and measured (symbols) Y_{22}-parameter vs. frequency for T_{chuck} = 25°C and for different electron cross section parameters (σ_n). Bias conditions: V_{DS} = 30 V and I_D = 57 mA.

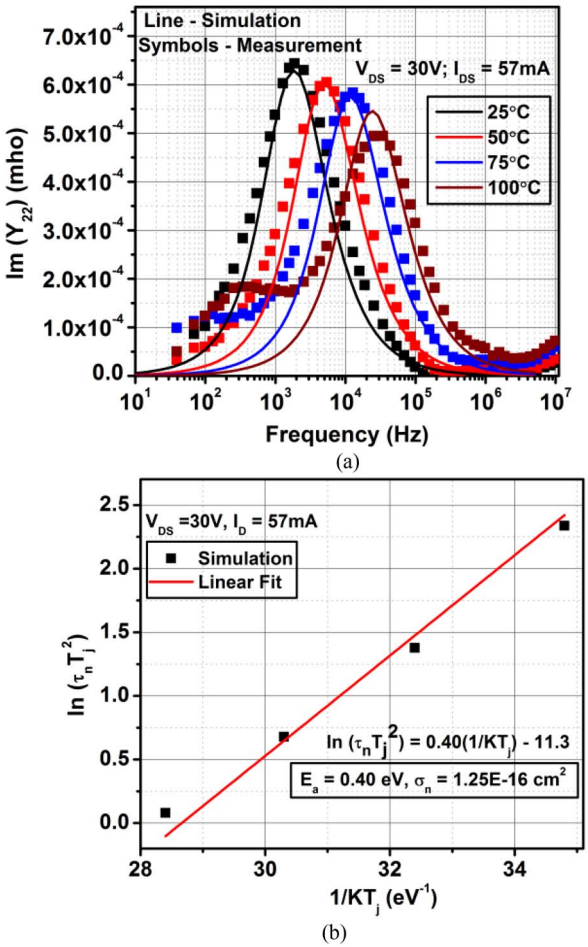

FIGURE 5. (a) Imaginary part of the simulated (lines) and measured (symbols) Y_{22}-parameter vs. frequency for the T_{chuck} ranges between 25°C and 100°C. Bias conditions: V_{DS} = 30 V and I_D = 57 mA. (b) Extracted Arrhenius plot using the simulated Y_{22}-parameter.

and for varying T_{chuck} between 25°C and 125°C. The good agreement between the simulation results and the measured data confirms the validity of the TCAD simulation model calibration.

Using the calibrated TCAD simulation model, LF admittance parameters simulation has been carried out at bias conditions of V_{DS} = 30 V and I_D = 57 mA. The self-heating effect of the device has been taken into account by extracting the thermal resistance (R_{TH}) of the device using the method described in [21]. The extracted R_{TH} of the device is 20.42°C/W. Thus, by knowing the R_{TH} value,

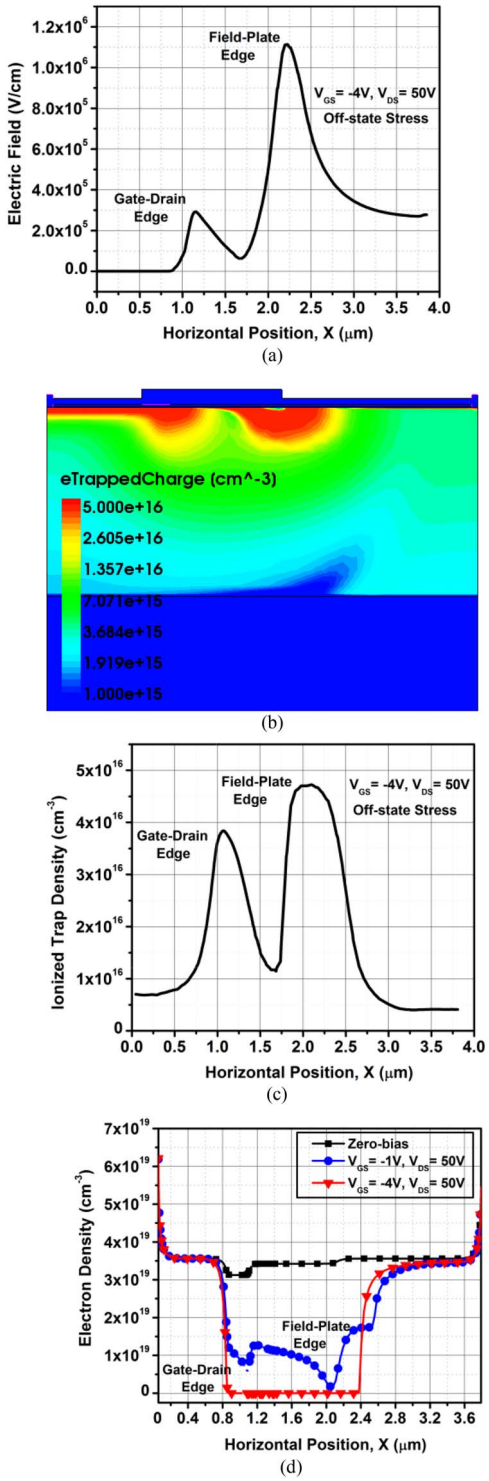

FIGURE 6. TCAD simulation results of AlGaN/GaN HEMT under off-state stress conditions (V_{DS} = 50 V and V_{GS} = -4 V). (a) Electric field profile (b) Ionized acceptor traps density profile (c) Ionized trap density distribution through the GaN buffer layer (d) Electron distribution through the GaN buffer layer for zero bias (V_{DS} = V_{GS} = 0 V) and different gate bias conditions.

the T_{chuck} and the power dissipation (P_{diss}), the junction temperature (T_j) has been estimated for different T_{chuck} and are used in simulations. Fig. 4 shows the simulated Y_{22} parameter for different electron cross section parameters (σ_n) and for T_{chuck} = 25°C. The σ_n value of 3.2 × 10^{-18}cm^2 yields an excellent match between the measured and simulated Y_{22} parameters over the temperature range of 25°C to 125°C. Therefore, this particular value of σ_n is used in all our TCAD physical simulations. Fig. 5 (a) shows the comparison of the simulated and measured imaginary part of the Y_{22} parameter for the frequency range of 10 Hz to 10 MHz and for various T_{chuck}. A good agreement obtained between the TCAD simulations and measurements confirms the presence of acceptor-like traps in the GaN buffer of the device. To the best of our knowledge, this is the first time that such a comparison between the simulated and measured Y_{22} parameter has been reported for the GaN HEMT device technology. Fig. 5(b) shows the Arrhenius plot extracted using the simulated Y_{22} parameter. The extracted trap energy level is 0.4 eV which corresponds to the acceptor trap energy level value introduced in the physical simulation.

The device is biased into off-state stress conditions (V_{DS} = 50 V and V_{GS} = -4 V, below pinch-off) in order to analyze the electric field profile in the device. The electric field obtained from the TCAD simulation is shown in Fig. 6(a). Two peaks are observed, i.e., one at the drain side edge of gate terminal and the other at the field-plate edge in gate-drain spacing region. Moreover, the electric field below the field-plate edge is higher than under the drain side gate edge [15]. The corresponding ionized trap charge density profile is shown in Fig. 6 (b). It can be observed that maximum trapping (Fig. 6 (b) and (c)) occurs below the field-plate edge where the electric field is maximum. Furthermore, these ionized acceptor traps depletes the 2DEG in the channel. The corresponding simulated electron density in the channel region for different device biases is shown in Fig. 6 (d). It could be concluded that trapping occurs both under the drain side of gate edge and field-plate edge.

D. IDENTIFICATION OF AlGaN BARRIER TRAPS

Fig. 7 (a) shows the imaginary part of the simulated Y_{22} parameter when both the acceptor-like and donor-like traps are introduced in the AlGaN barrier. Acceptor-like traps are placed at 0.6 eV below the conduction band whereas donor-like traps are placed at 0.3 eV below the conduction band. The assumed trap concentration (N_T) is 1 × 10^{16} cm^{-3} and the electron and hole cross sections are assumed to be σ_n = 1 × 10^{-18} cm^2 and σ_p = 1 × 10^{-20} cm^2, respectively. The traps introduced in the AlGaN barrier does not cause any dispersion in the simulated Y_{22} parameter. Moreover, when the traps are introduced in both the AlGaN barrier (both acceptor and donor-like traps) and GaN buffer (N_T = 5 × 10^{16} cm^{-3}, E_{TA} = 0.4 eV), dispersion occurs in the simulated admittance parameter (Fig. 7 (b)) and the activation energy value extracted from the Arrhenius plot (Fig. 7 (c)) corresponds to the trap energy level value used in the GaN buffer. This result demonstrates that AlGaN barrier traps cannot be identified using this method. However, traps in

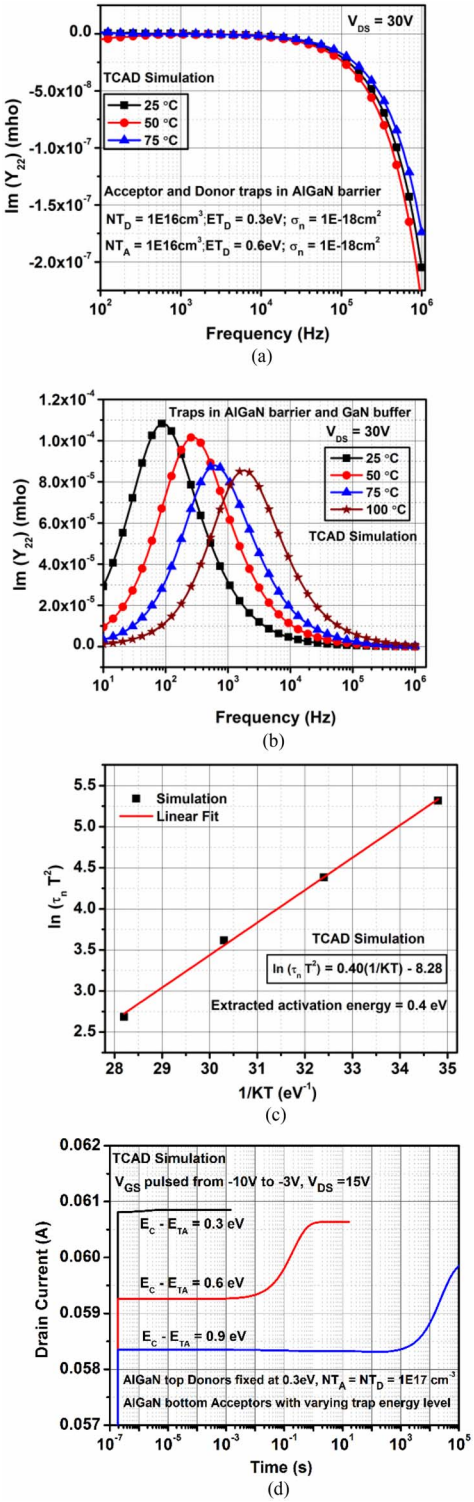

FIGURE 7. Imaginary part of the simulated Y_{22}-parameter vs. frequency for different T_{chuck}. (a) Traps in the AlGaN barrier. (b) Traps in both AlGaN barrier and GaN buffer. (c) Extracted Arrhenius plot using simulated Y_{22}-parameter. (d) Simulated gate-lag transient characteristics with acceptor and donor-like traps in the AlGaN barrier.

the AlGaN barrier can be identified via different measurement techniques such as gate/drain lag transients. Fig. 7 (d) shows the simulated transient characteristics of the device when the gate is pulsed from -10 V to -3 V and the drain voltage is fixed at 15 V. Donor-like traps are introduced in the AlGaN barrier at the specified energy level of 0.3 eV below the conduction band. Similarly, acceptor-like traps are placed at the bottom region of AlGaN barrier which is close to the GaN channel. Traps energy level (E_{TA}) is considered as a varying parameter to study the influence of energy level of traps on transient characteristics. It can be clear from the Fig. 7 (d) that the traps introduced in the AlGaN barrier capture electrons from the channel and therefore, the drain current remains at a lower value for some period until the traps start to re-emit the captured electrons. Moreover, deeper the energy level of acceptor-like traps, more the possibility of ionization of acceptors, larger the time required to reach the steady state drain current. Furthermore, the donor-like traps has less influence (verified using several simulations) on the simulated transient characteristics as they are located away from the channel. This result suggests that traps in the AlGaN barrier can be identified using gate-lag measurements.

IV. CONCLUSION

In this work, we have extracted the activation energy and cross section of traps present in the GaN buffer of the GaN/AlGaN/GaN HEMT device using LF S-parameter measurements. Moreover, we have also presented the TCAD physical simulation results for this device. The TCAD physical simulation model has been calibrated and then, LF admittance simulations have been performed. A good agreement has been achieved between the simulated and measured Y_{22} parameter. This strongly suggests that LF admittance measurement is an effective tool for characterizing GaN buffer traps. Furthermore, our simulation results reveal that traps in the AlGaN barrier can be identified using gate/drain lag transient measurements. Therefore, the simulation results presented here establish a correlation with measurements in order to identify the location of traps and this could provide an efficient feedback for further improving the GaN HEMT technology and its respective RF performance.

REFERENCES

[1] U. K. Mishra, L. Shen, T. E. Kazior, and Y.-F. Wu, "GaN-based RF power devices and amplifiers," *Proc. IEEE*, vol. 96, no. 2, pp. 287–305, Feb. 2008.

[2] R. S. Pengelly, S. M. Wood, J. W. Milligan, S. T. Sheppard, and W. L. Pribble, "A review of GaN on SiC high electron-mobility power transistors and MMICs," *IEEE Trans. Microw. Theory Techn.*, vol. 60, no. 6, pp. 1764–1783, Jun. 2012.

[3] B. Lu and T. Palacios, "High breakdown (>1500 V) AlGaN/GaN HEMTs by substrate-transfer technology," *IEEE Electron Device Lett.*, vol. 31, no. 9, pp. 951–953, Sep. 2010.

[4] J. G. Felbinger *et al.*, "Comparison of GaN HEMTs on diamond and SiC substrates," *IEEE Electron Device Lett.*, vol. 28, no. 11, pp. 948–950, Nov. 2007.

[5] Y.-F. Wu, M. Moore, A. Saxler, T. Wisleder, and P. Parikh, "40-W/mm double field-plated GaN HEMTs," in *Proc. 64th Device Res. Conf.*, State College, PA, USA, 2006, pp. 151–152.

[6] J. W. Chung, W. E. Hoke, E. M. Chumbes, and T. Palacios, "AlGaN/GaN HEMT with 300-GHz f_{max}," *IEEE Electron Device Lett.*, vol. 31, no. 3, pp. 195–197, Mar. 2010.

[7] Y. Tang *et al.*, "Ultrahigh-speed GaN high-electron-mobility transistors with f_T/f_{max} of 454/444 GHz," *IEEE Electron Device Lett.*, vol. 36, no. 6, pp. 549–551, Jun. 2015.

[8] J. S. Moon *et al.*, "Gate-recessed AlGaN-GaN HEMTs for high-performance millimeter-wave applications," *IEEE Electron Device Lett.*, vol. 26, no. 6, pp. 348–350, Jun. 2005.
[9] D. Jin and J. A. del Alamo, "Methodology for the study of dynamic ON-resistance in high-voltage GaN field-effect transistors," *IEEE Trans. Electron Devices*, vol. 60, no. 10, pp. 3190–3196, Oct. 2013.
[10] J. Yang *et al.*, "Electron tunneling spectroscopy study of electrically active traps in AlGaN/GaN high electron mobility transistors," *Appl. Phys. Lett.*, vol. 103, no. 22, 2013, Art. no. 223507.
[11] J. Joh and J. A. del Alamo, "A current-transient methodology for trap analysis for GaN high electron mobility transistors," *IEEE Trans. Electron Devices*, vol. 58, no. 1, pp. 132–140, Jan. 2011.
[12] G. Meneghesso *et al.*, "Reliability issues of gallium nitride high electron mobility transistors," *Int. J. Microw. Wireless Technol.*, vol. 2, no. 1, pp. 39–50, Feb. 2010.
[13] M. Silvestri, M. J. Uren, and M. Kuball, "Iron-induced deep-level acceptor center in GaN/AlGaN high electron mobility transistors: Energy level and cross section," *Appl. Phys. Lett.*, vol. 102, no. 7, 2013, Art. no. 073501.
[14] J.-C. Nallatamby *et al.*, "A microwave modeling oxymoron?: Low-frequency measurements for microwave device modeling," *IEEE Microw. Mag.*, vol. 15, no. 4, pp. 92–107, Jun. 2014.
[15] W.-C. Liao, J.-I. Chyi, and Y.-M. Hsin, "Trap-profile extraction using high-voltage capacitance–voltage measurement in AlGaN/GaN heterostructure field-effect transistors with field plates," *IEEE Trans. Electron Devices*, vol. 62, no. 3, pp. 835–839, Mar. 2015.
[16] J. Hu, S. Stoffels, S. Lenci, G. Groeseneken, and S. Decoutere, "On the identification of buffer trapping for bias-dependent dynamic R_{ON} of AlGaN/GaN Schottky barrier diode with AlGaN:C back barrier," *IEEE Electron Device Lett.*, vol. 37, no. 3, pp. 310–313, Mar. 2016.
[17] C. Potier *et al.*, "Highlighting trapping phenomena in microwave GaN HEMTs by low-frequency S-parameters," *Int. J. Microw. Wireless Technol.*, vol. 7, nos. 3–4, pp. 287–296, Jun. 2015.
[18] N. K. Subramani *et al.*, "Characterization of parasitic resistances of AlN/GaN/AlGaN HEMTs through TCAD-based device simulations and on-wafer measurements," *IEEE Trans. Microw. Theory Techn.*, vol. 64, no. 5, pp. 1351–1358, May 2016.
[19] O. Ambacher *et al.*, "Two-dimensional electron gases induced by spontaneous and piezoelectric polarization charges in N-and Ga-face AlGaN/GaN heterostructures," *J. Appl. Phys.*, vol. 85, no. 6, pp. 3222–3233, 1999.
[20] W. D. Hu *et al.*, "Self-heating simulation of GaN-based metal-oxide-semiconductor high-electron-mobility transistors including hot electron and quantum effects," *J. Appl. Phys.*, vol. 100, no. 7, Oct. 2006, Art. no. 074501.
[21] A. K. Sahoo *et al.*, "Thermal analysis of AlN/GaN/AlGaN HEMTs grown on Si and SiC substrate through TCAD simulations and measurements," in *Proc. EUMW*, London, U.K., Oct. 2016, pp. 145–148.

NANDHA KUMAR SUBRAMANI received the M.E. degree in VLSI design from the College of Engineering Guindy, Anna University, Chennai, India, in 2012, and the M.Phil. degree in electronic and electrical engineering from the University of Sheffield, Sheffield, U.K., in 2015. He is currently pursuing the Ph.D. degree in RF and microwave characterization with the XLIM Laboratory, University of Limoges, France.

His current research interests include microwave characterization and modeling, physics-based device simulation and analytical modeling of GaN HEMTs.

JULIEN COUVIDAT received the master's degree in electronic engineering from the University of Bordeaux, Bordeaux, France, in 2015. He is currently pursuing the Ph.D. degree with a joint doctoral degree programme between XLIM Laboratory, University of Limoges, France, and the IMS Laboratory, University of Bordeaux.

His research interests include GaN microwave power devices characterization and high power amplifiers architectures for airborne systems.

AHMAD AL HAJJAR received the master's degree and the Ph.D. degree in electronics from the University of Limoges, Limoges, France, in 2012 and 2016, respectively, where he is currently a Post-Doctoral Researcher.

His current research interests include low frequency characterization of noise in a semiconductor, microwave characterization, and modeling of power devices, particularly GaN-based HEMTs and heterojunction bipolar transistors.

JEAN-CHRISTOPHE NALLATAMBY received the Ph.D. degree in electronics from the University of Limoges, Limoges, France, in 1992, where he is currently a Professor. His current research focuses on the microwave, low frequency noise characterization and modeling of high speed semiconductor devices, characterization of charge-trapping effects in GaN HEMTs, and understanding its physical behaviour using TCAD based device simulation.

RAPHAEL SOMMET received the French aggregation degree in applied physics in 1991 and the Ph.D. degree from the University of Limoges, Limoges, France, in 1997. Since 1997, he has been a Permanent Researcher with the CNRS (French National Research Center), XLIM Laboratory, C^2S^2 Team "Nonlinear Microwave Circuits and Subsystems." His research interests concern physics-based device simulation, 3-D thermal finite element simulation, thermal measurements and modeling, model order reduction, microwave circuit simulation, and generally the coupling of all physics-based simulation with circuit simulation.

RAYMOND QUÉRÉ (F'09) received the Ph.D. degree in electrical engineering from the University of Limoges, Limoges, France, in 1989, where he was appointed as a Full Professor in 1992. From 1998 to 2013, he led the Department of High Frequency Devices, Circuits, Signals and Systems, XLIM Laboratory, CNRS, University of Limoges, where he has been the Deputy Director of the XLIM Laboratory since 2013. His research interests include modeling and design of nonlinear circuits for telecommunications and radar systems. He has authored or co-authored over 300 publications in international journals, international, and national conferences. He was appointed as a General Chairman of the European Microwave Week in 2005. He is the holder of the Chair "Design of future integrated smart RF transceivers (DEFIS-RF)" funded by Thales Alenia Space, Thales Corporation and the French Research Agency.